Pergamon

Adv. Space Res. Vol. 18, No. 11, pp. (11)195–(11)201, 1996

0273–1177/96 $15.00 + 0.00

PII: S0273–1177(96)00019–1

PARTICLE RADIATION EFFECTS ON AND CALIBRATION OF SPACE INFRARED DETECTORS

G. Roth, J. Wolf and D. Lemke

Max-Planck-Institut für Astronomie, Königstuhl 17, 69117 Heidelberg, Germany

ABSTRACT

The far-infrared detectors of ESA's ISO satellite are sensitive enough to allow measurements at the limits imposed by the natural sky background. However, high-energy protons and electrons of the earth's radiation belts induce spikes, higher dark current and detector noise as well as an increased level of responsivity. These effects cause signal drifting for hours after the belt passage, resulting in a temporary loss of the detectors' photometric calibration.

The passage of the ISOPHOT detectors through the radiation belts has therefore been simulated in the laboratory and effective curing methods searched for to restore the detectors' photometric calibration. With a combination of bright IR-flashes of the ISOPHOT onboard calibration source and a bias boost the detectors can now be reset to within a few percent of the pre-irradiation characteristics.

KEYWORDS: Infrared Space Observatory (ISO), ISOPHOT, infrared detectors, high-energy radiation effects, curing, IR-flash, bias boost

1. INTRODUCTION

The ISO FIR satellite will be launched in September 1995 to observe a large variety of astronomical objects between 2.5 and 240 μm. Telescope and experiments of the satellite are cooled down to 2-3 K with a supply of 2300 l of superfluid helium. The life time of ISO is expected to exceed 18 months. One of ISO's focal plane instruments is ISOPHOT, which contains photometric, spectrometric and imaging capabilities in three detector groups PHT-P, PHT-S and PHT-C. The single-pixel units and detector arrays are made of Si:Ga, Si:B, Ge:Ga and stressed Ge:Ga [4]. Table 1 gives some detector characteristics.

Table 1 : ***Photodetectors used in ISOPHOT***

Instrument	Detector	Material	Wavelength [μm]
PHT-P1	single detector	Si:Ga	3...19
PHT-P2	single detector	Si:B	9...29
PHT-P3	single detector	Ge:Ga	37...129
PHT-S1	array (64 pixels)	Si:Ga	6.0...12.0
PHT-S1	array (64 pixels)	Si:Ga	2.5...5.0
PHT-C100	3 x 3 pixel	Ge:Ga	37...129
PHT-C200	2 x 2 pixel	stressed Ge:Ga	58...242

ISO's 24h orbit is a very eccentric ellipse with a perigee of 1,000 km and an apogee of 70,500 km. This keeps the satellite within the earth's radiation belts for 6 hours a day (3 before and 3 after perigee). These belts consist of high-energy protons (inner belt) and electrons (outer belt) with typical proton energies of between 10 and 200 MeV, and up to 7 MeV for electrons.The satellite walls and local shielding function as absorbers for the high-energy particles, reduce their velocity and may eventually trap them. Therefore only protons with energies of $E > 80$ MeV can reach the IR detectors, whereas electrons are absorbed in the outer parts of the satellite, and only bremsstrahlung photons can interact with the detectors, mainly via Compton scattering. The expected mission dose rate for 18 months in orbit is $D = 2$ krad [1,2].

Protons and bremsstrahlung photons can ionise lattice atoms of the detectors, which produces free electron-hole-pairs, and they can remove lattice atoms, creating irreversible crystal defects. Estimates show, however, that the number of additionally created defects is negligible compared to the impurity concentration in a typical lattice.

Therefore the aim was to simulate the ionising effects of the belt passage in the laboratory (compare Fig. 1.1). For all experiments a ^{137}Cs source with an activity of A = 2.1 GBq was used, which emits photons with an energy of E = 662 keV. A cryostat with replica models of the respective detector unit and the possibility of inserting different band pass filters in the beam path of the internal IR-source TRS (Thermal Radiation Source) was used. An external black body in combination with different cold neutral filters was also applied. All the tests were performed under nominal ISO operating conditions. During γ-irradiation the Cs-source was located outside the cryostat, which exposed the detectors to a dose rate of D = ~ 0.6 rad/h. Because of the expected orbit dose of D = 3.7 rad [3] an irradiation period of ~ 6 hours could be calculated. After 30-40 min of irradiation the effects on the semi-conductor became saturated and continued irradiation did not change the detector characteristics any further [6]. This can also be explained theoretically [8].

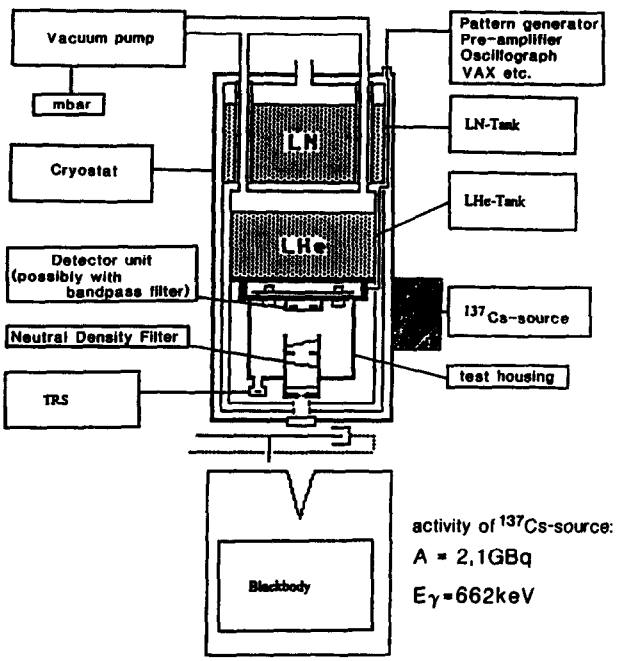

Fig. 1.1 : Test equipment for irradiation tests. The cryostat contains a replica model (RM) of the ISOPHOT detectors, different cold filters and an internal radiation source TRS. An external black body beam can also be applied. During γ-exposure the Cs-source was located near the cryostat walls. Most of the experiments were carried out with the Ge:Ga detectors PHT-C100RM, PHT-P3RM and PHT-C200RM.

2. RADIATION EFFECTS ON ISOPHOT MEASUREMENTS

The measurements during and immediately after γ-exposure were seen to contain spikes - sudden increases of detector current, when the detector is hit by a γ-quantum -, which lead to an increase of detector noise by several orders of magnitude.

Fig. 2.1 shows the CRE (Cold Read-Out Electronic) of ISOPHOT. The detector is AC-coupled to an integrating amplifier and its photo-current charges the feedback capacitor C_F. The integrated charge is transfered by a SAMPLE pulse to the sample & hold stage and then read out through the multiplexer (non-destructive readout). If a RESET pulse follows the SAMPLE, the integration of the front-end amplifier starts over (destructive readout). Each detector input channel contains a front-end integrator and a sample & hold stage. In Fig. 2.2 a typical signal output with multiple non-destructive readouts between resets is shown. The detector signal is calculated as the mean slope of the integration ramps and the noise is the standard deviation of the slopes. At the end of the measurement in figure 2.2 a spike occurs. This test sequence was measured shortly after irradiation, where occasional spikes can be removed by deglitching software routines. During irradiation, however, each ramp contains more than one spike, which leads to highly increased detector noise and makes measurements during irradiation useless.

In addition the dark current is greatly increased after irradiation due to produced free charge carriers, which create a detector signal without any IR-flux. Fig. 2.3 shows the dark current signal of the P3RM-detector before and after a 40 min irradiation period, where dark current increases from a few mV/sec up to S = 0.5 V/sec. The signal is very unstable and drifts slowly back to the pre-irradiation value.

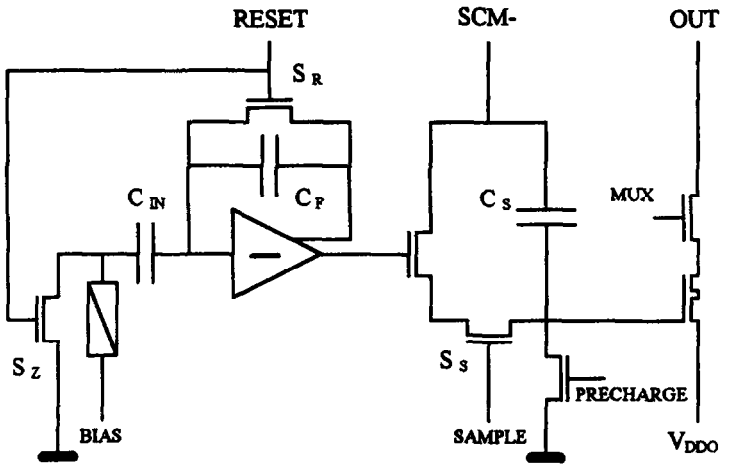

Fig. 2.1: ISOPHOT Cold Readout Electronics (CRE).
Up to 66 detector input cells, each containing an integrating amplifier and sample&hold stage, are integrated in a monolithic CMOS chip. All integrated signals are multiplexed into a single output line. In a low power dissipating "standby" mode, both switches S_Z and S_R are closed.

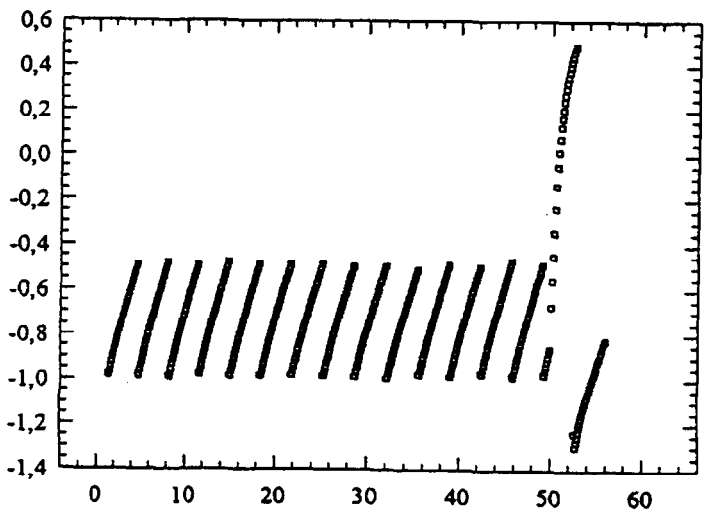

Fig. 2.2:
CRE Integration Ramps
This measurement was done a few seconds after a γ-irradiation, while the detector was still spiking.

The most important irradiation effect, however, is the increase of detector signal as compared to pre-exposure and therefore a change of detector responsivity R. This can be explained by recombination processes of produced free electron-hole-pairs with detector impurities, which change the trap concentration and consequently the life time of IR-produced free holes [5]. Fig. 2.4 shows the increase of detector signal after irradiation for the P3RM-detector. The two different signals refer to two different IR-fluxes on the detector. A second plot (Fig. 2.5) shows the signal difference in percent compared to the non-irradiated values. It can be seen that the signals increase up to a factor of 30 and then show drifts with relaxation times of many hours.

Changes of detector signal and noise coincide with changes of responsivity and NEP. Fig. 2.6 shows R and NEP of the C100RM detector before and after irradiation. Responsivity increases up to a factor of 4 can be observed, but this situation is not stable, because R drifts for a long time. Therefore irradiation leads to a loss of detector calibration. Also the noise-to-signal-ratio (NEP) is increased. But in contrast to R, the NEP reaches the pre-irradiation value one hour after γ-exposure, whereas R needs many hours to recover. Therefore curing methods are necessary in order to speed up recovery. As long as R is increased, observa-

tions of bright IR-objects could function as an additional curing and change detector calibration. This is why curing should be as complete as possible.

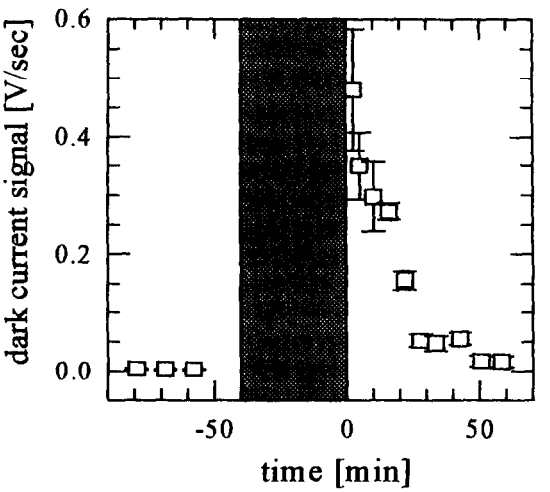

Fig. 2.3 : *Dark current signal of the P3RM detector before and after a 40 min irradiation period (crosshatched) with a total dose of D = 0.4 rad. The signal is increased from several mV/sec up to S = 0.5 V/sec, behaves in a very unstable way and drifts slowly back to the pre-irradiation value.*

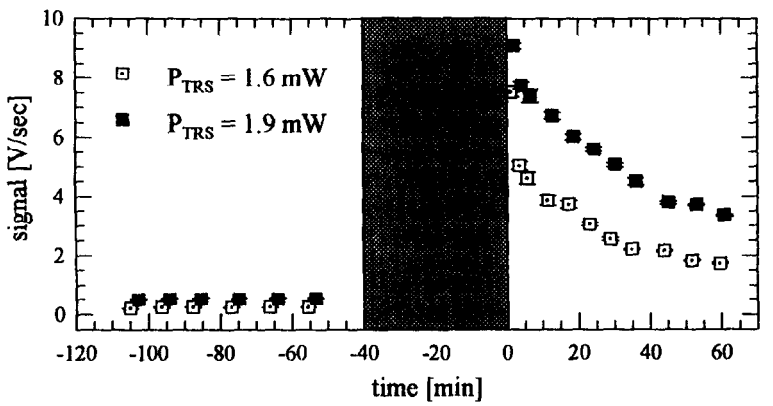

Fig. 2.4 : *Signal of P3RM of two different IR-fluxes produced by the TRS before and after irradiation with D = 0.4 rad (crosshatched).*

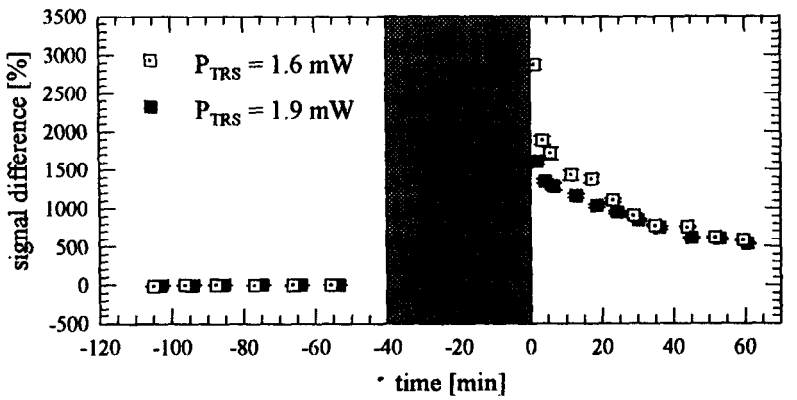

Fig. 2.5 : *Signal difference in percent. The signal is increased up to a factor of 30 compared to the one calculated from the mean of the pre-irradiation values and keeps on drifting. The relaxation time involves many hours, because one hour after irradiation the signals are still a factor of 5 higher than before irradiation.*

3. OPTIMISED CURING RESULTS FOR PHT-C100RM, -P3RM and -C200RM

There are several possible curing methods which restore detector calibration. Although self-relaxation is possible theoretically, the relaxation time would be too long, and observers would have to wait for many hours until a stable signal was reached. A first curing method, the increase of temperature (thermal curing), is not applicable for ISOPHOT's Ge:Ga detectors, because they are coupled directly to the LHe-tank of the satellite. Possible methods for ISOPHOT are the increase of detector voltage until the detectors are in break-through-condition (bias boost) or illumination with a bright IR-beam (IR-flash).

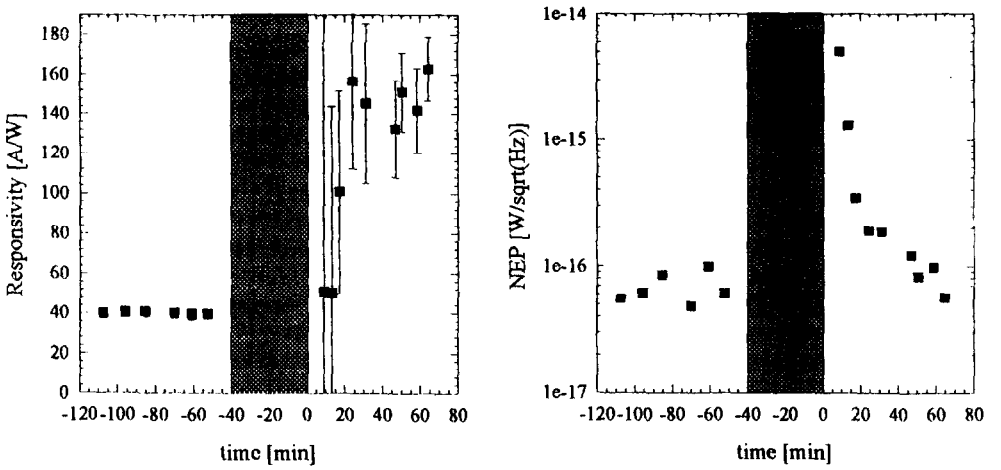

Fig. 2.6 : *R and NEP of C100RM before and after irradiation with D = 0.4 rad. NEP increases up to two orders of magnitude, but reaches the original values 1 hour after irradiation. In contrast to this R - increased by a factor of 4 after γ-exposure - behaves in a very unstable way and drifts for hours. Therefore curing is necessary to restore detector calibration, whereas detector sensitivity (NEP) shows "self-curing".*

The different curing methods have been tested for the PHT Ge:Ga detectors and found to be effective using a combination of bias boosts and IR-flashes. Optimisation of the different curing parameters was also tried. This included the optimised flashing time as well as flashing power, boost voltage and the application of the standby mode, where the reset switches of the CRE are closed, and the detector is connected directly to the ground (compare Fig. 2.1).

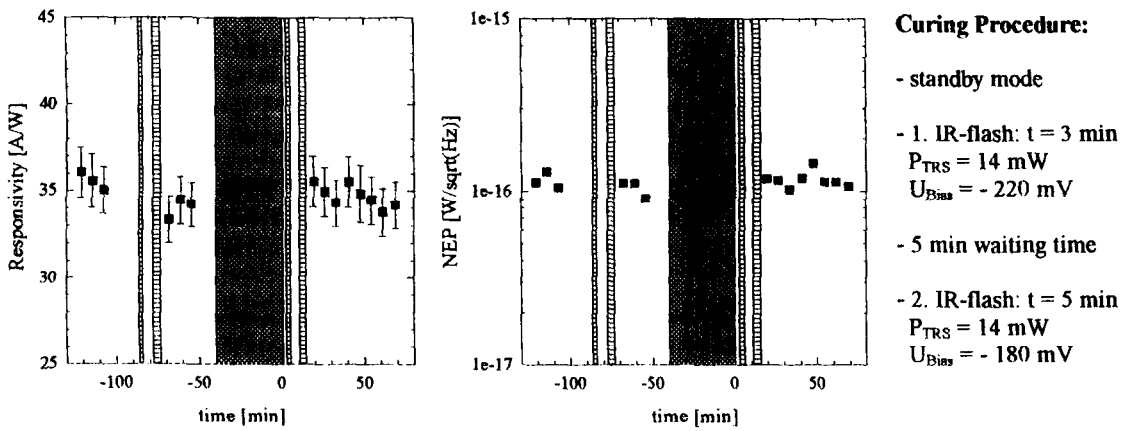

Fig. 3.1 : *R and NEP of C100RM before and after irradiation (crosshatched) and curing with a 3 min boost/flash-combination and after a 5 min waiting time another 5 min IR-flash (horizontal lines). Both R and NEP reached their pre-irradiation values. The error bars of the responsivity are due to error propagation.*

During standby mode the detector current was three times as high as usual, which makes curing much more effective. Fig. 3.1 shows responsivity and NEP after applying the optimised curing procedure for the C100RM detector (U_{Bias} = - 180 mV; T = 3.0 K) with a 60μm bandpass installed in the light beam. We were able to reduce the flashing time to 3 minutes for the boost/flash-combination and to 5 minutes for the second IR-flash. The exact curing parameters are given on the right hand side. The waiting time between the two flashes can be used to flash another detector, which leads to an effective flashing time of only 8 minutes.

Figure 3.2 shows curing for the P3RM detector (U_{Bias} = - 260 mV; T = 2.9 K) with the same 60μm bandpass inserted in the beam path of the TRS as for the C100RM unit. It was not necessary to increase the duration of the flashes, but rather to apply higher IR-fluxes to obtain satisfying results. It can be seen that after this modification of the curing procedure all signals reach their pre-irradiation level to within a few percent.

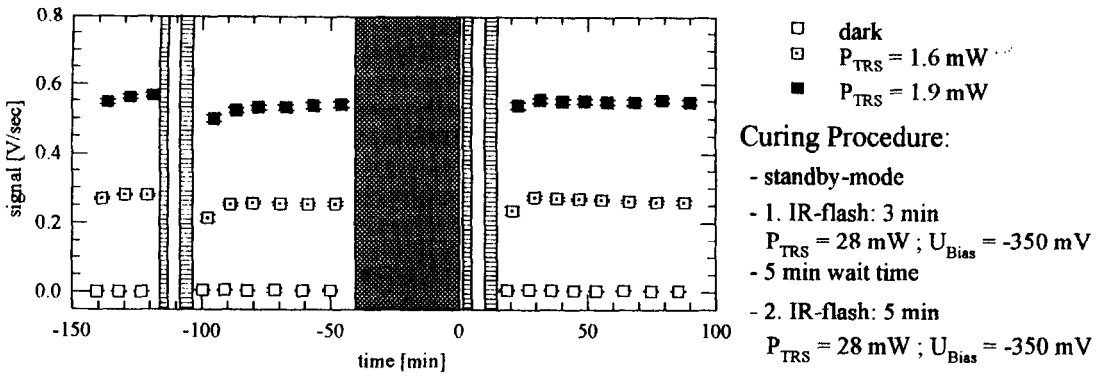

Fig. 3.2. : *Dark current and two different detector signals before and after irradiation (crosshatched) and curing with a 3 min boost/flash-combination and after a waiting time of 5 min a second 5 min IR-flash (horizontal lines). In contrast to the PHT-C100RM curing method, here the power of the flashes had to be increased. The pre-irradiation values are reached within 3-5 %.*

Finally, figure 3.3 shows the results for the C200RM detector (U_{Bias} = - 80 mV; T = 1.8 K), where instead of a bandpass a quartz windows was inserted in the beam path, which will also be possible in the flight instruments. Here we had to encrease the duration of the flashes to 5 and 10 minutes, which leads to satisfactory results for the stressed Ge:Ga detector as well.

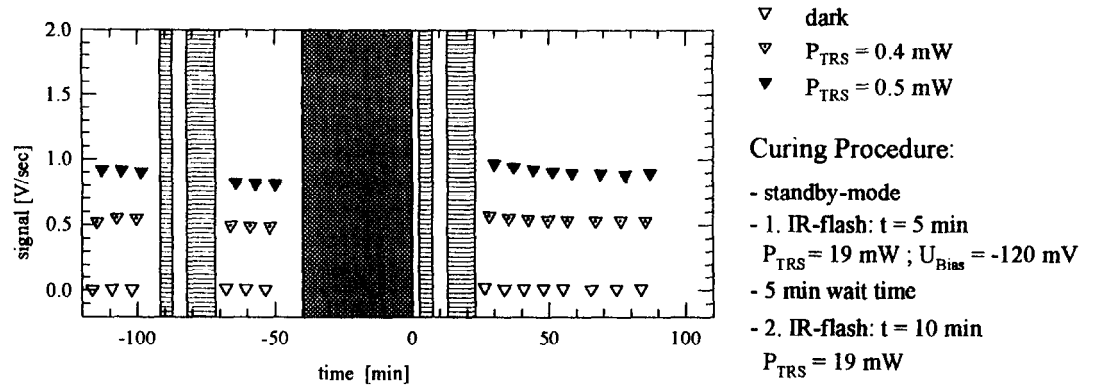

Figure 3.3 : *Optimised curing procedure for C200RM (stressed Ge:Ga). The detector seemed to be more affected by irradiation than the unstressed material, and we therefore had to encrease the duration of the flashes from 3 to 5 and from 5 to 10 minutes (horizontal lines). Finally the signal reached the original values to within a few percent after a total flashing time of only 15 minutes.*

4. CONCLUSIONS

We found curing procedures for all ISOPHOT Ge:Ga detectors, which restore detector sensitivity and calibration to within a few percent after a total flashing time of only 8 and 15 minutes respectively. The exact curing parameters are summarised in Table 4.1 [7]. This is short enough to allow PHT to fit into the so-called activation window of about one hour, the time between switch-on of the satellite after the belt passage and the beginning of the observing time. Recently an activation sequence has been worked out which includes all the steps necessary to switch on and cure the detectors and to get ready for measurements. This sequence contains the optimised boost/flash-combinations for the Ge:Ga detectors and thermal annealing for the silicon detectors [9].

Test sequences were also started to examine whether irradiation effects accumulate after more than one irradiation period and orbit simulations, which should represent dose profile during the first hours after perigee in a more realistic way, by reducing the dose rate to four steps. Fortunately neither was accumulation observed nor was curing less effective after orbit simulations. The first orbits of the performance verification phase will establish whether or not our experiments were a realistic simulation of the ISO orbit.

	C100RM	P3RM	C200RM
nominal operating parameters	T = 3.0 K U_{Bias} = -180 mV	T = 2.9 K U_{Bias} = -260 mV	T = 1.8 K U_{Bias} = -80 mV
cold filters	60μm bandpass	60μm bandpass	quartz window
standby mode	during whole curing procedure	during whole curing procedure	during whole curing procedure
1. IR-flash	U_{Bias} = -220 mV P_{TRS} = 14 mW S = (378 ± 9) V/sec Φ = (5.71 ± 0.06) $.10^{-13}$ W/pixel t = 3 min	U_{Bias} = -350 mV P_{TRS} = 28 mW S = (377 ± 8) V/sec Φ = (1.17 ± 0.09) $.10^{-12}$ W/pixel t = 3 min	U_{Bias} = -120 mV P_{TRS} = 19 mW S > 900 V/sec Φ > 10^{-11} W/pixel t = 5 min
waiting time	5 min	5 min	5 min
2. IR-flash	U_{Bias} = -180 mV P_{TRS} = 14 mW S = (260 ± 7) V/sec Φ = (5.71 ± 0.06) $.10^{-13}$ W/pixel t = 5 min	U_{Bias} = -350 mV P_{TRS} = 28 mW S = (377 ± 8) V/sec Φ = (1.17 ± 0.09) $.10^{-12}$ W/pixel t = 5 min	U_{Bias} = -80 mV P_{TRS} = 19 mW S > 900 V/sec Φ > 10^{-11} W/pixel t = 10 min

Table 4.1 : *Optimised curing parameters for the ISOPHOT Ge:Ga detectors. In orbit the detectors will be flashed by the on-board calibration source FCS.*

5. ACKNOWLEDGEMENTS

The ISOPHOT project is funded by Deutsche Agentur für Raumfahrtangelegenheiten (DARA) in Bonn and supported by several collaborating institutes in Denmark, Spain and the UK. The industrial development was performed at Dornier, Carl Zeiss, Batelle, IMEC and CASA. We would like to thank U. Grözinger, Max-Planck-Institut für Astronomie, for his support throughout laboratory tests and calibration measurements of ISOPHOT.

6. REFERENCES

[1] ESA : *Bremsstrahlung Photon Modelling for the ISO 24h-Orbit*, (1987)

[2] ESA : *ISO Call for Experiment and Mission Scientist Proposals*, SCI (84) 1, ESA Blue Book, Annex 1 and 4 (1984)

[3] ESA : *ISO System Radiation Analysis*, ISO.AS.14:TN.0169, ESA-Aerospatiale (1989)

[4] Lemke, D. et al. : *ISOPHOT - Far-infrared Imaging, Polarimetry and Spectrophotometry on the Infrared Space Observatory*, Optical Engineering, Vol. 33, No.1 (1994)

[5] Petroff, M. D. et al. : *Low-Level Radiation Effects in* Extrinsic *Infrared Detectors*, IEEE Transactions on Nuclear Sciences, NS 26-6, 4840 (1979)

[6] Roth, G. : *Untersuchung von Strahlenschäden und Ausheilmethoden an (Ge:Ga)-Infrarotdetektoren*, diploma thesis, Max-Planck-Institut für Astronomie, Heidelberg (1994)

[7] Schubert, J., Roth, G., Wolf, J., Lemke, D., Fouks, B. I. : *Correction and Curing of In-Orbit Induced Non-Ideal Behaviour of ISOPHOT's Photodetectors*, SPIE Proc. 2268-30 (1994)

[8] Varnell, L. : *Radiation Effects in IRAS Extrinsic Infrared Detectors*, IEEE Transactions on Nuclear Sciences, Vol. NS-29, No. 6, (1982)

[9] Wolf, J., Lützow-Wentzky, P., Grözinger, U., Patrashin, M., Roth, G. : *High-Energy Radiation Effects and Curing of ISOPHOT Photodetectors - Proposal for a ISOPHOT Curing Sequence*, internal paper, Max-Planck-Institut für Astronomie, Heidelberg (1993)